

Research Article

Xianghong Meng, Yu Zhang*, Duoyun Wang, and Xue Zhang

Provenance analysis of the Late Triassic Yichuan Basin: constraints from zircon U-Pb geochronology

<https://doi.org/10.1515/geo-2018-0003>

Received Oct 31, 2017; accepted Jan 09, 2018

Abstract: Laser ablation inductively coupled plasma mass spectrometry (LA-ICP-MS) U-Pb dating has been performed on detrital zircons from the Chunshuyao Formation sandstone of Yichuan Basin. The ages of 85 detrital zircon grains are divided into three groups: 252–290 Ma, 1740–2000 Ma, and 2400–2600 Ma. The lack of Early Paleozoic and Neoproterozoic U-Pb ages indicates that there is no input from the Qinling Orogen, because the Qinling Orogen is characterized by Paleozoic and Neoproterozoic material. In combination with previous research, we suggest that the source of the Chunshuyao Formation is most likely recycled from previous sedimentary rocks from the North China Craton. In the Late Triassic, the Funiu ancient land was uplifted which prevented source material from the Qinling Orogen. Owing to the Indosinian orogeny, the strata to the east of the North China Craton were uplifted and eroded. The Yichuan Basin received detrital material from the North China Craton.

Keywords: Yichuan Basin; Late Triassic; Detrital zircon; Provenance

1 Introduction

The Triassic is a significant period in the evolution of sedimentary basins in northern China. In the Triassic, the western Henan region was a large depression basin. In the early

Cenozoic, due to the differential uplift and fault depression that occurred in the area, several faulted basins were formed on the Triassic prototype basin (Luoyang Basin, Yichuan Basin, Linru Basin). The Yichuan Basin is a part of the Southern North China Basins in the southern margin of the North China Craton (NCC) which exposes some Triassic strata and provides favorable conditions for us to study the Triassic strata in the southern margin of the NCC. At present, study of the Yichuan Basin is mainly confined to the structural characteristics of the source rock properties [1–5]. Study of the formation and evolution of the Upper Triassic crushed rock in the Yichuan Basin is limited. There are two main aspects of the study controversy at present: (1) whether the Qinling Orogen is a substantial source of uplift for the Upper Triassic strata; and (2) whether there is a paleo-uplift between the Qinling Orogen and the Yichuan Basin in the Triassic. These controversies limit our understanding of the evolution of the southern margin and Qinling Orogen of the NCC. In this study, the LA-ICP-MS method was used to determine the U-Pb age of zircons from the sandstone of the Upper Triassic Chunshuyao Formation in the Yichuan Basin, western Henan. The age characteristics of the zircons in the Yichuan Basin were analyzed, and a paleogeographic reconstruction was performed.

2 Geological Setting

The Yichuan Basin lies on the western margin of the NCC. It belongs to the Mesozoic inner continental sedimentary basin. The tectonic system changes in the Yichuan Basin are closely related to the Qinling-Dabie Orogenic belt, the Taihang orogen, and the Tanlu fault [5]. As it was in phase with the northern margin of the North China Plate and Yangtze plate, which is the convergent part of a variety of stress produced by the tectonic movement between the Taihang orogenic belt and the east Qinling-Dabie orogenic belt, which resulted in multi-stage tectonic evolution. The Yichuan Basin is a Meso-Cenozoic superimposed basin de-

***Corresponding Author: Yu Zhang:** School of Marine Sciences, Guangxi University, Nanning 530004, China; Guangxi Laboratory on the Study of Coral Reefs in the South China Sea, Nanning 530004, China; Coral Reef Research Center of China, Guangxi University, Nanning 530004, China; Email: hyzhangyu@gxu.edu.cn

Xianghong Meng, Duoyun Wang: Faculty of Geographical Science, Beijing Normal University, Beijing 100875, China

Xue Zhang: The School of Earth Science and Resources, Chang'an University, Xi'an, 710054, China

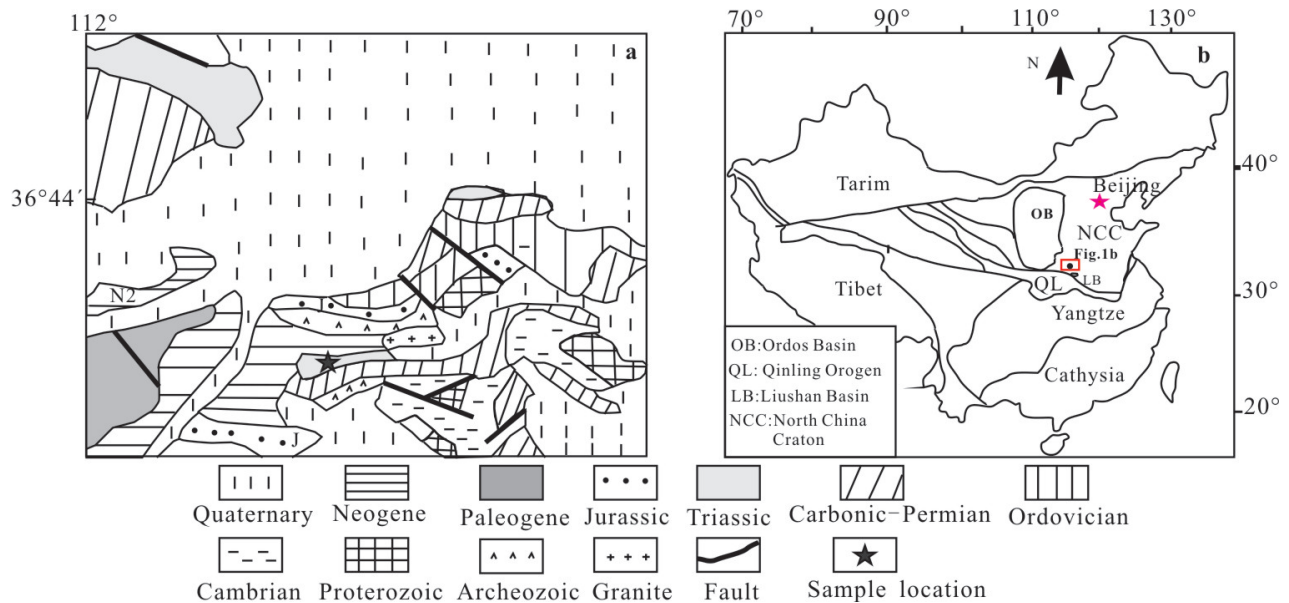


Figure 1: Geological map of Yichuan Basin

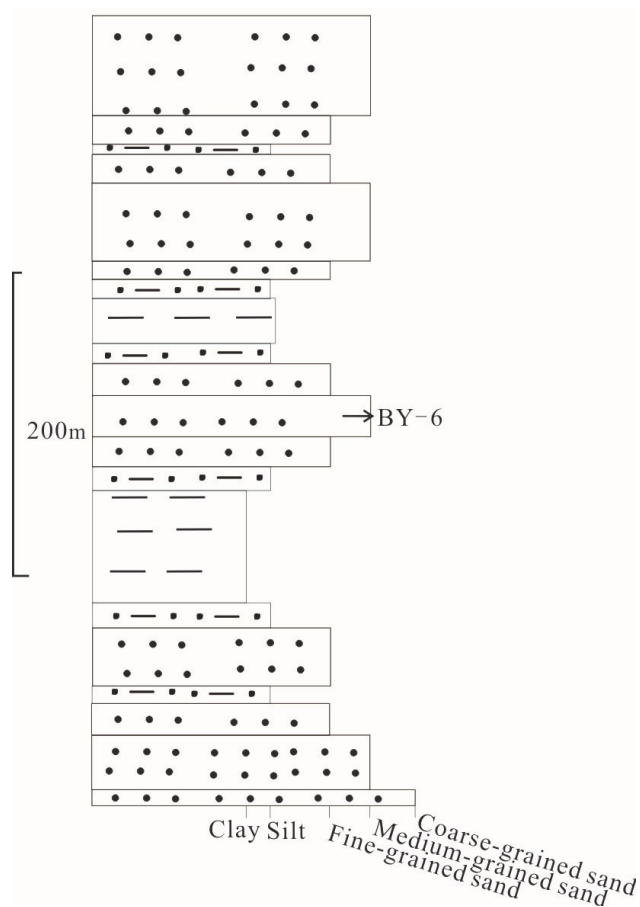


Figure 2: Sedimentological profile of the Chunshuyao Formation from Yichuan basin

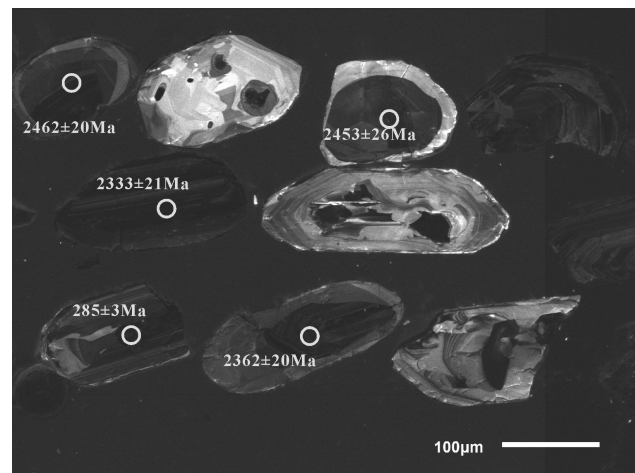


Figure 3: Cathodoluminescence images of selected zircons

veloped on the North China Platform, showing an overall NW trending. The southwest margin is defined by the Funiushan uplift. The southeast margin is bordered by the Songshan uplift. The basement of the Yichuan Basin is mainly composed of Precambrian metamorphic crystalline basement rock. The strata is well developed. Exposed strata in the study area include the Precambrian, Paleozoic, Triassic, Jurassic, Paleogene, Neogene and Quaternary (Figure 1).

The Upper Triassic strata are the main target horizons for oil and gas exploration in the Yichuan Basin. The Upper Triassic succession includes the Chunshuyao Formation at the base and the Tanzhuang Formation at the top. The Chunshuyao Formation is a set of lacustrine fa-

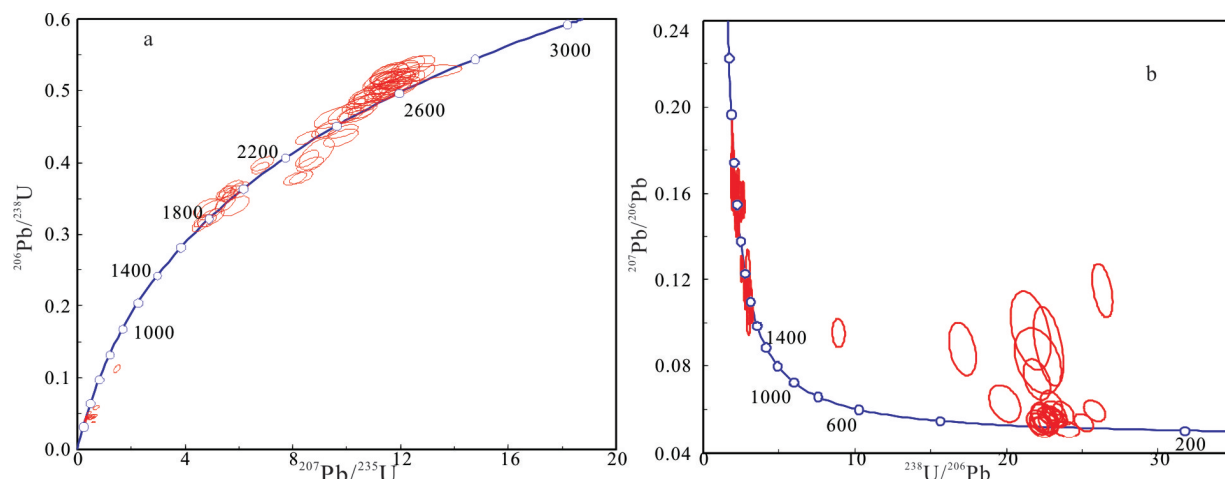


Figure 4: a: U–Pb concordia diagrams of detrital zircon analyses. b: Tera–Wasserburg concordia diagram of detrital zircon analyses

cies, mainly composed of feldspar sandstone and mudstone (Figure 2). The Tanzhuang Formation is a set of lacustrine-marsh facies, which are mainly composed of yellow-green, purple-red, gray-green clay rock and gray-yellow feldspar quartzite. Our study focused on the Upper Triassic Chunshuyao Formation of the Yichuan Basin. A sample of medium to coarse-grained sandstone was collected for detrital zircon age analysis.

3 Analytical procedures

3.1 Sample preparation

Detrital zircons were separated from a 4 kg rock sample using conventional heavy liquid and magnetic techniques, and then purified by hand-picking under a binocular microscope at the Langfang Regional Geological Survey, Hebei Province, China. The detailed analysis process is as follows: before being comminuted, the rock samples were cleaned by tap water. Then, the samples were broken into pieces of several millimeters in size by using a jaw breaker, and were washed in tap water again and dried in the air. A rotary disc mill was used and the rock pieces were milled into powder and sifted through sieve cloths of ca. 150 μm in pore size. The initial density separation was performed using an oscillating table. Then, using a hand magnet, any highly magnetic grains were removed, followed by magnetic separation using a Frantz isodynamic separator. The zircons were picked up under a binocular microscope. More than 150 grains were randomly selected from the sample, affixed on epoxy resin, together with the standard samples, and polished to about half their thickness.

Zircon Cathodoluminescence (CL) images were obtained at the Beijing Geoanalytical Co., Ltd., Beijing, China, using an Analytical Scanning Electron Microscope (JSM-6510.cl) connected to a GATAN MINICL system, in order to observe internal textures of crystals and to select potential target sites.

3.2 Zircon U–Pb Dating

U–Pb dating of zircon was conducted by the laser inductively coupled plasma mass spectrometer (LA-ICP-MS) at the State Key Laboratory of Geological Processes and Mineral Resources, China University of Geosciences, Wuhan. Detailed operating conditions for the laser ablation system and the ICP-MS instrument and data reduction are the same as those described by Liu *et al.* [6–8]. Laser sampling was conducted using a 193 nm GeoLas 2005 laser-ablation system with a spot size of 32 μm . An Agilent 7500a ICP-MS instrument was used to acquire ion-signal intensities. Each analysis incorporated an approximately 20-second background acquisition (gas blank) followed by 50 seconds of data acquisition from the sample. Zircon 91500 [9] was used as the external standard for age calculation and re-analyzed after every 6 analyses of the detrital zircon grains. NISTSRM610 was analyzed twice every 24 analyses for U, Th, and Pb concentration calculations. Off-line selection and integration of background and analyte signals, time-drift correction and quantitative calibration were performed by ICPMSDataCal [6, 7]. Common Pb corrections were done by the following the method of Anderson [10]. Age calculations and the plotting of concordia diagrams were done using ISOPLOT programs [11].

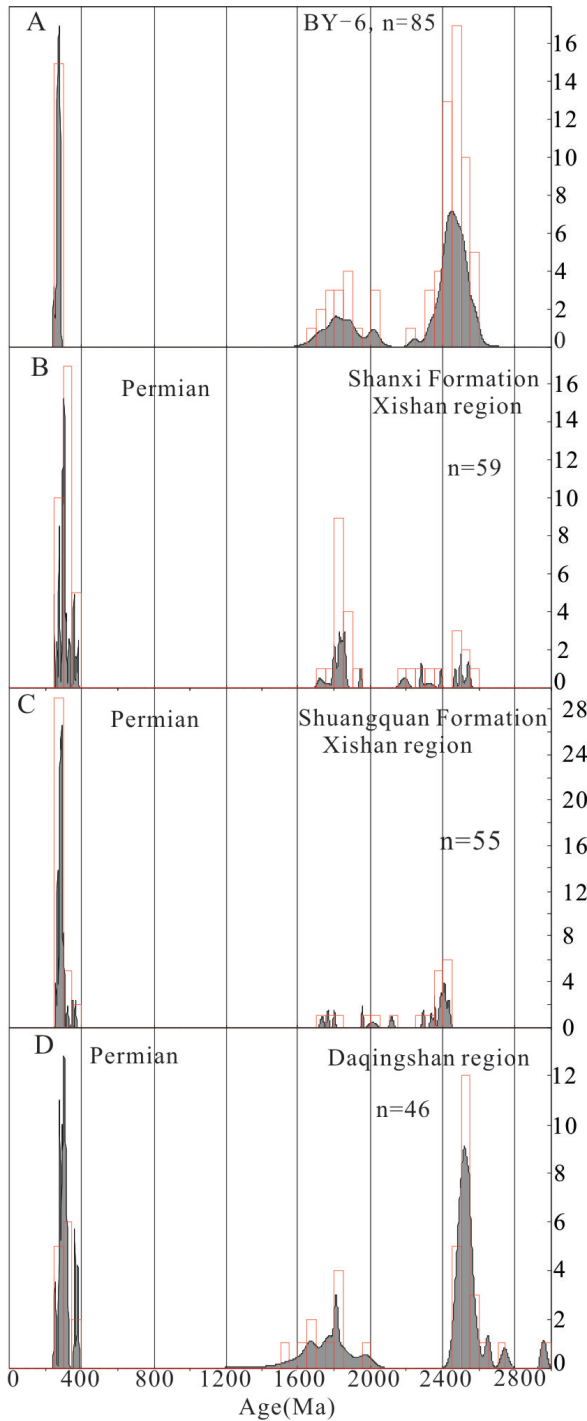


Figure 5: Comparison of detrital zircon ages from Yichuan basin with counterparts from the North China Craton (Data sources are [50, 51]). A: Relative probability density diagram of ages for the sample BY-6; B: Relative probability density diagram of ages for the Shanxi Formation from the Xishan region; C: Relative probability density diagram of ages for the Shuangquan Formation from the Xishan region; D: Relative probability density diagram of ages for the Permian section from the Daqingshan region

The exact number of grains necessary for a provenance study is a controversial topic. Dodson *et al.* considered 60 grains to be sufficient [12]. Vermeesch suggested that at least 117 grains should be dated [13], whereas Anderson [10] believed that 35-70 grains would be adequate if the grains are randomly analyzed. In this study, we followed Anderson's suggestion.

4 Results

The CL images are shown in Figure 3, part of the zircon developing magma-type oscillatory zoning. The zircon grains show a rounded-circular shape, reflecting their long-distance handling and abrasion or multiple-stage depositional recirculation. U-Pb ages have been determined for 96 detrital zircon grains from the BY-6. U-Pb ages are listed in Table 1. Zircon grains are from euhedral prismatic and acicular to subhedral stubby and anhedral elliptical and rounded in morphology, with grain sizes varying from 50 to 150 μm (Figure 3). Th/U ratios of zircons range from 0.33 to 1.48, consistent with a magmatic origin [14]. Because $^{206}\text{Pb}/^{238}\text{U}$ ages are generally more precise for younger zircons whereas $^{207}\text{Pb}/^{206}\text{Pb}$ ages are more precise for older zircons, $^{206}\text{Pb}/^{238}\text{U}$ ages were used for grains which are younger than 1000 Ma, and $^{207}\text{Pb}/^{206}\text{Pb}$ ages for grains which are older than 1000 Ma [15]. All analyses are shown on concordia plots (Figure 4).

However, analyses yielding data less than 90% concordant were not included in the frequency diagrams (Figure 5). As a result, BY-6 has an available age number of 85. As shown in Figure 5, the detrital zircon U-Pb age patterns show a wide range, indicating that there is a great variety of rocks in the source areas. The age population is grouped into three major age ranges: 290-252 Ma, 2000-1740 Ma, and 2600-2400 Ma.

5 Discussion

5.1 Potential Source Areas

Since the debris sedimentary rocks cannot produce zircon during the deposition process, the zircon particles mainly come from the weathered parent rock. Based on the accurate measurement of the formation time of the detrital zircons in the basin and the surrounding geological exposition, it is possible to determine the composition information of the rock in the provenance area. The source of the clastic sedimentary rocks mainly includes magmatic

Table 1: LA-ICP-MS U-Pb analysis of zircons from Chunshuyao Formation sandstone (BY-6) in Yichuan basin

Spots	Element (ppm)		Th/U	Isotopic ratios (1σ)				Apparent ages (Ma)				Concordance				
	Th	U		²⁰⁷ Pb/ ²⁰⁶ Pb	1σ	²⁰⁷ Pb/ ²³⁵ U	1σ	²⁰⁶ Pb/ ²³⁸ U	1σ	²⁰⁷ Pb/ ²⁰⁶ Pb	1σ	²⁰⁷ Pb/ ²³⁵ U	1σ	²⁰⁶ Pb/ ²³⁸ U	1σ	
BY-6-01	90.7	100	0.91	0.1092	0.0050	4.9817	0.2095	0.3347	0.0056	1786	52	1816	36	1861	27	97%
BY-6-02	374	1850	0.20	0.1597	0.0037	9.8618	0.2281	0.4436	0.0039	2453	27	2422	21	2367	17	97%
BY-6-03	64.5	134	0.48	0.1025	0.0041	4.7565	0.1884	0.3372	0.0052	1670	50	1777	33	1873	25	94%
BY-6-04	388	861	0.45	0.1660	0.0037	11.9018	0.2703	0.5145	0.0048	2518	26	2597	21	2676	20	97%
BY-6-05	1011	966	1.05	0.1134	0.0029	5.7906	0.1452	0.3666	0.0036	1855	31	1945	22	2013	17	96%
BY-6-06	403	1727	0.23	0.1237	0.0032	6.8821	0.1769	0.3987	0.0040	2010	31	2096	23	2163	18	96%
BY-6-07	1052	2551	0.41	0.0537	0.0019	0.3369	0.0118	0.0451	0.0005	358	57	295	9	284	3	96%
BY-6-08	325	512	0.63	0.1574	0.0037	10.8893	0.2655	0.4957	0.0055	2427	26	2514	23	2595	24	96%
BY-6-09	44.5	161	0.28	0.1633	0.0046	11.6054	0.3239	0.5116	0.0065	2490	30	2573	26	2663	28	96%
BY-6-10	220	375	0.59	0.0535	0.0032	0.3311	0.0187	0.0450	0.0007	349	99	290	14	284	4	97%
BY-6-11	2284	2276	1.00	0.1535	0.0033	8.0861	0.1769	0.3777	0.0037	2385	24	2241	20	2066	17	91%
BY-6-12	190	236	0.80	0.0640	0.0041	0.4343	0.0285	0.0503	0.0011	743	103	366	20	316	7	85%
BY-6-13	452	512	0.88	0.1642	0.0038	11.3108	0.2616	0.4945	0.0045	2499	27	2549	22	2590	19	98%
BY-6-14	356	586	0.61	0.1112	0.0026	5.5794	0.1328	0.3599	0.0035	1819	29	1913	20	1982	16	96%
BY-6-15	388	362	1.07	0.1488	0.0034	9.2017	0.2038	0.4445	0.0042	2333	25	2358	20	2371	19	99%
BY-6-16	108	217	0.50	0.1688	0.0043	12.5206	0.3102	0.5346	0.0059	2546	27	2644	23	2761	25	95%
BY-6-17	184	1302	0.14	0.1521	0.0036	9.9303	0.2541	0.4673	0.0061	2370	26	2428	24	2472	27	98%
BY-6-18	1363	1459	0.93	0.0589	0.0024	0.3165	0.0123	0.0387	0.0004	564	65	279	9	245	3	86%
BY-6-19	537	961	0.56	0.1630	0.0041	11.7491	0.3010	0.5166	0.0057	2487	28	2585	24	2685	24	96%
BY-6-20	937	628	1.49	0.0847	0.0069	0.5398	0.0502	0.0439	0.0008	1309	155	438	33	277	5	54%
BY-6-21	845	1416	0.60	0.1607	0.0031	10.6013	0.2197	0.4730	0.0049	2463	21	2489	19	2497	22	99%
BY-6-22	60.2	99.5	0.60	0.1113	0.0046	4.9588	0.2006	0.3237	0.0052	1820	50	1812	34	1808	25	99%
BY-6-23	197	167	1.18	0.1674	0.0043	11.6813	0.2988	0.5028	0.0062	2531	27	2579	24	2626	27	98%
BY-6-24	280	549	0.51	0.1655	0.0037	11.8599	0.2738	0.5145	0.0052	2512	25	2593	22	2676	22	96%
BY-6-25	309	178	1.73	0.1598	0.0041	10.6329	0.2669	0.4809	0.0059	2453	26	2492	23	2531	26	98%
BY-6-26	395	583	0.68	0.1412	0.0030	8.5244	0.1753	0.4345	0.0037	2242	24	2289	19	2326	17	98%
BY-6-27	236	238	0.99	0.1672	0.0038	11.9798	0.2889	0.5152	0.0058	2529	25	2603	23	2679	25	97%
BY-6-28	199	759	0.26	0.1640	0.0035	11.5801	0.2572	0.5079	0.0051	2497	24	2571	21	2648	22	97%
BY-6-29	1982	3029	0.65	0.0512	0.0019	0.2920	0.0103	0.0417	0.0006	249	54	260	8	263	4	98%
BY-6-30	579	757	0.76	0.1622	0.0041	9.7876	0.2601	0.4343	0.0050	2479	29	2415	24	2325	22	96%
BY-6-31	261	534	0.49	0.1595	0.0039	10.3494	0.2632	0.4676	0.0050	2450	29	2467	24	2473	22	99%
BY-6-32	422	640	0.66	0.1563	0.0035	10.7038	0.2481	0.4932	0.0050	2416	26	2498	22	2584	22	96%
BY-6-33	532	651	0.82	0.0584	0.0029	0.3451	0.0166	0.0432	0.0006	544	81	301	13	273	4	90%
BY-6-34	102	213	0.48	0.1089	0.0032	4.8147	0.1404	0.3191	0.0035	1782	37	1787	25	1785	17	99%
BY-6-35	527	361	1.46	0.1578	0.0035	11.2190	0.2549	0.5129	0.0055	2432	24	2541	21	2669	23	95%
BY-6-36	1504	1048	1.43	0.1604	0.0036	11.2784	0.2620	0.5066	0.0051	2460	26	2546	22	2642	22	96%
BY-6-37	1243	1596	0.78	0.0538	0.0020	0.2958	0.0106	0.0398	0.0004	362	62	263	8	252	3	95%
BY-6-38	710	1695	0.42	0.1730	0.0032	12.0820	0.2233	0.5043	0.0045	2586	19	2611	17	2632	19	99%
BY-6-39	1100	1073	1.03	0.1604	0.0028	10.7854	0.2103	0.4846	0.0050	2460	19	2505	18	2547	22	98%

Continued on next page

Table 1: ... continued

Spots	Element (ppm)		Th/U	Isotopic ratios (1 σ)				Apparent ages (Ma)				Concordance	
	Th	U		$^{207}\text{Pb}/^{235}\text{U}$	$^{206}\text{Pb}/^{238}\text{U}$	$^{207}\text{Pb}/^{206}\text{Pb}$	$^{207}\text{Pb}/^{235}\text{U}$	$^{207}\text{Pb}/^{206}\text{Pb}$	$^{207}\text{Pb}/^{235}\text{U}$	$^{206}\text{Pb}/^{238}\text{U}$	1σ	1σ	1σ
BY-6-40	282	194	1.45	4.6135	0.1155	0.3192	0.0035	1709	30	1752	21	1786	17
BY-6-41	170	181	0.94	4.5753	0.1267	0.3143	0.0043	1740	31	1745	23	1762	21
BY-6-42	671	644	1.04	10.8636	0.2441	0.4939	0.0049	2442	25	2512	21	2588	21
BY-6-43	493	2597	0.19	5.4534	0.1170	0.3581	0.0037	1796	24	1893	18	1973	18
BY-6-44	3029	1955	1.55	0.6025	0.0302	0.0380	0.0004	1861	76	479	19	240	3
BY-6-45	220	350	0.63	11.3934	0.2223	0.5224	0.0057	2430	19	2556	18	2710	24
BY-6-46	212	676	0.31	11.1819	0.2106	0.5147	0.0047	2420	20	2538	18	2677	20
BY-6-47	302	1700	0.18	10.3126	0.1994	0.4788	0.0040	2403	21	2463	18	2522	18
BY-6-48	420	748	0.56	0.0559	0.0031	0.0445	0.0006	448	98	299	14	281	4
BY-6-49	1013	2054	0.49	0.1556	0.0029	0.0488	0.0046	2408	21	2486	18	2565	20
BY-6-50	727	1337	0.54	0.0559	0.0021	0.0431	0.0005	450	83.3	293	9.3	272	2.9
BY-6-51	180	423	0.43	12.2857	0.2548	0.5348	0.0051	2511	22	2626	19	2762	22
BY-6-52	593	993	0.60	10.1398	0.2044	0.4662	0.0041	2418	22	2448	19	2467	18
BY-6-53	223	372	0.60	11.5736	0.2805	0.5239	0.0063	2450	25	2571	23	2716	27
BY-6-54	424	489	0.87	0.0555	0.0037	0.0444	0.0007	433	112	297	16	280	4
BY-6-55	764	2045	0.37	0.1567	0.0035	0.0487	0.0039	2420	27	2486	21	2548	17
BY-6-56	1541	775	1.99	0.1577	0.0033	0.3795	0.0036	2431	23	2267	19	2074	17
BY-6-57	1160	2146	0.54	0.0570	0.0018	0.0433	0.0004	491	49	298	8	273	3
BY-6-58	3123	2218	1.41	0.1515	0.0028	0.4052	0.0049	2363	20	2290	19	2193	22
BY-6-59	190	391	0.49	0.0736	0.0043	0.0454	0.0008	1030	96	386	19	286	5
BY-6-60	197	368	0.53	0.1598	0.0038	0.5231	0.0058	2453	26	2573	23	2712	24
BY-6-61	155	164	0.95	0.0858	0.0083	0.0457	0.0013	1333	128	421	31	286	8
BY-6-62	1234	1550	0.80	0.1606	0.0030	0.5149	0.0048	2462	20	2567	18	2678	20
BY-6-63	492	2593	0.19	0.1489	0.0028	0.3123	0.0050	2333	21	2369	19	2385	22
BY-6-64	467	1737	0.27	0.0518	0.0019	0.0451	0.0005	276	63	285	9	285	3
BY-6-65	654	1715	0.38	0.0523	0.0019	0.3242	0.0015	300	60	285	9	282	3
BY-6-66	224	219	1.02	0.0900	0.0064	0.0473	0.0012	1426	95	543	28	366	8
BY-6-67	794	894	0.09	0.1729	0.0085	0.5239	0.0047	2586	74	2657	48	2716	20
BY-6-68	701	1009	0.69	0.0538	0.0024	0.3269	0.0005	362	77	287	11	278	3
BY-6-69	180	423	0.43	0.1650	0.0035	0.120902	0.0055	2508	22	2611	20	2723	23
BY-6-70	396	962	0.41	0.1593	0.0031	0.5281	0.0050	2448	21	2566	18	2692	21
BY-6-71	328	481	0.68	0.1633	0.0036	0.5006	0.0049	2490	23	2556	20	2616	21
BY-6-72	1044	997	1.05	0.1115	0.0027	0.5278	0.0036	1824	29	1905	21	1962	17
BY-6-73	43.5	92.3	0.47	0.1483	0.0045	0.5115	0.0061	2327	35	2389	28	2451	27
BY-6-74	904	1823	0.50	0.0555	0.0019	0.3269	0.0004	431	52	287	8	269	3
BY-6-75	1160	2606	0.45	0.1536	0.0029	0.8843	0.0090	2386	24	2326	27	2224	41
BY-6-76	90.6	155	0.58	0.1725	0.0044	12.5070	0.0059	2582	27	2643	24	2714	25
BY-6-77	279	416	0.67	0.1644	0.0038	11.4991	0.0048	2501	26	2565	22	2629	21
BY-6-78	685	808	0.85	0.0628	0.0027	0.3772	0.0164	700	71	325	12	275	3

Continued on next page

Table 1: ... continued

Spots	Element (ppm)		Th/U	Isotopic ratios (1 σ)			Apparent ages (Ma)			Concordance	
	Th	U		$^{207}\text{Pb}/^{235}\text{U}$	1 σ	$^{206}\text{Pb}/^{238}\text{U}$	1 σ	$^{207}\text{Pb}/^{235}\text{U}$	1 σ	$^{206}\text{Pb}/^{238}\text{U}$	1 σ
BY-6-79	251	180	1.39	0.0959	0.0084	0.6148	0.0548	0.0463	0.0012	1545	130
BY-6-80	325	585	0.56	0.1649	0.0035	11.3854	0.2442	0.4968	0.0045	2507	24
BY-6-81	259	303	0.86	0.1682	0.0036	11.8277	0.2506	0.5069	0.0048	2540	23
BY-6-82	595	1483	0.40	0.1245	0.0024	6.8013	0.1337	0.3926	0.0033	2021	23
BY-6-83	190	1055	0.18	0.1150	0.0024	5.6554	0.1231	0.3537	0.0035	1879	25
BY-6-84	275	387	0.71	0.1707	0.0041	12.1866	0.2979	0.5140	0.0059	2564	26
BY-6-85	383	385	1.00	0.1159	0.0028	5.7584	0.1381	0.3581	0.0041	1894	27
BY-6-86	248	223	1.12	0.1153	0.0031	5.4857	0.1530	0.3429	0.0046	1885	31
BY-6-87	129	122	1.06	0.1252	0.0045	5.8655	0.2154	0.3395	0.0056	2031	42
BY-6-88	355	313	1.13	0.1630	0.0036	11.2806	0.2530	0.4985	0.0055	2487	23
BY-6-89	573	1694	0.34	0.0576	0.0021	0.3478	0.0117	0.0440	0.0005	514	54
BY-6-90	660	1836	0.36	0.1566	0.0037	8.6552	0.2063	0.3977	0.0042	2419	26
BY-6-91	2548	4760	0.54	0.0578	0.0016	0.3478	0.0096	0.0435	0.0005	521	42
BY-6-92	152	1262	0.12	0.0933	0.0026	1.4719	0.0515	0.1122	0.0021	1495	38
BY-6-93	786	1215	0.65	0.0582	0.0025	0.3389	0.0143	0.0421	0.0005	537	72
BY-6-94	361	439	0.82	0.1718	0.0036	12.0932	0.2607	0.5072	0.0049	2575	23
BY-6-95	242	975	0.25	0.1190	0.0027	6.0185	0.1418	0.3646	0.0035	1941	28
BY-6-96	74.5	294	0.25	0.1635	0.0041	11.9285	0.3122	0.5263	0.0063	2492	28

Concluded

rocks, metamorphic rocks and recycled rock complexes of old crustal sections [16, 17]. The North China Craton (NCC), the Inner Mongolia Paleo-uplift, the Qinling Orogen, and the pre-Middle Triassic sediments of the North China Craton constitute the potential source areas for the Yichuan Basin during the Late Triassic.

The Qinling Orogen lies to the south of the Yichuan Basin. It is characterized by Lower Paleozoic igneous rocks [18–24]. In addition, there are some Mesozoic and Neoproterozoic rocks [18, 25–28]. The North Qinling Ocean closed in the Early Paleozoic, and an Early Paleozoic volcanic arc was formed along the area from Qinling to Dabie at the southern margin of the NCC [29, 30]. In the Indosinian, the unroofing pattern of Qinling Orogen developed by denudation of sediments from young covers to old basements [31].

In the NCC, 1.8 Ga and 2.5 Ga are the primary age populations. On the basis of our present state of knowledge, the ~2500 and ~1800 Ma tectonothermal events are typically attributed to the NCC [32–34]. The 2.5 Ga material can be found throughout the NCC. It is a rapid accretionary period of the crustal growth in North China. A large number of magmatic activities occur, which can be used as an important sign of the end of the Archean cratonization in North China [35–39]. The ~1.8 Ga tectonothermal event may represent the collision between the Eastern and Western blocks to form the NCC [38–43], and it is characterized by anorogenic magmatism, rift-magmatism or volcanism, and retrograde metamorphism [44, 45].

Late Paleozoic magmatic activity within the NCC occurs mainly in the Inner Mongolia Palaeo-uplift (IMPU) [46, 47]. The IMPU lies in the northern Yichuan Basin. It is a Late Palaeozoic Andean-style continental arc and characterized by Late Paleozoic magmatic activity [46]. During the Late Paleozoic to Early Mesozoic, the differential uplift and exhumation between the IMPU and the Yanshan fold-and-thrust was distinct. The strong uplift and exhumation of the IMPU occurred during the Late Paleozoic to Early Mesozoic. The strong differential uplift and erosion led to the lack of Mesoproterozoic-Paleozoic sedimentary rocks and the exhumation of the basement crystalline rocks [48, 49].

In addition, the pre-Middle Triassic sedimentary rocks of the NCC might be the potential sediment source for the Yichuan Basin in the Middle-Late Triassic. The Carboniferous to Permian strata from the northern margin of the NCC contain three groups of detrital zircons (260–380 Ma, 1500–1950 Ma, and 2400–2700 Ma) [50]. The Upper Carboniferous sandstone from the Ningwu Basin contains three groups of detrital zircons (300–320 Ma, 1600–2200 Ma, and 2300–2600 Ma) [30]. Yang *et al.* [51] showed that the Carbonif-

erous to Permian strata from the Xishan region had three major groups, 255–400 Ma, 1700–1950 Ma, and 2400–2550 Ma. Darby and Gehrels [33] reported that the upper Proterozoic to Ordovician strata from the northwestern Ordos Basin has two major age clusters, 1.8–2.1 and 2.5–2.8 Ga.

5.2 Detrital Zircon Provenance Analyses

The ages of the BY-6 were grouped into three major age ranges: 290–252 Ma, 2000–1740 Ma, and 2600–2400 Ma. The lack of Early Paleozoic and Neoproterozoic U-Pb ages indicates that there was no input from the Qinling Orogen, because the Qinling Orogen is characterized by Paleozoic and Neoproterozoic rocks [24, 25, 34, 52–54]. The youngest group of zircons (252–290 Ma) in the Yichuan Basin is concentrated in the Permian, corresponding to the Hercynian period. The Late Paleozoic magmatic activity was extensively developed in the IMPU [46, 47].

The youngest detrital zircon age of sample BY-6 is 252 ± 3 Ma, which is obviously older than deposition age of the Chunshuyao Formation (228–200 Ma), which indicates that this group of zircons cannot come from igneous rocks in the IMPU. U-Pb ages of the Phanerozoic zircons from the IMPU range from 395 to 107 Ma [50]; if the debris material comes from the northern margin of North China, its minimum deposition age should be close to the stratigraphic sedimentary age [51]. The composition of the detrital zircons in this study is similar to that of pre-Late Triassic sedimentary rocks, which indicates that the detrital material in the Chunshuyao Formation in the Yichuan Basin may come from pre-Late Triassic sedimentary rocks.

The two old groups are reflective of the provenance from the NCC basement, which records the collision between the Eastern and Western blocks to form the NCC and represents a rapid accretionary period of the crustal growth in North China [37–39]. The two groups of detrital zircons have been reported in the North China Craton sedimentary strata. Taking into account the zircon morphology (darker and rounded), we infer that the two old age groups were recycled from previous sedimentary rocks.

In the field survey, we measured the paleocurrent of the Chunshuyao Formation in the Yichuan Basin. The average paleocurrent of the sediment in the Yichuan basin was 258° , indicating that the sediments were from the northeastern part of the basin. Previous studies have pointed out that the eastern NCC uplifted and eroded in the Late Triassic due to the collision between the Yangtze Plate and the North China Plate [55–57]. It is further proved that Yichuan Basin received the recycled sediments from the central-eastern NCC in the Late Triassic. The Qinling

Orogen did not provide provenance for the Yichuan Basin in the Late Triassic.

5.3 Tectonic significance

Previous studies showed that the Ordos Basin extended eastward to the western Henan in the Triassic [57–59]. The detrital zircons U-Pb age from the lower Yanchang Formation in the southern Ordos Basin were grouped into three major age ranges: 363–238 Ma, 2.1–1.5 Ga, 2.6–2.2 Ga, and were mainly derived from recycled sediments [60], which is similar to our study. Accordingly, we can carry out paleogeographic reconstruction. During the Late Triassic, the Ordos Basin and the Yichuan Basin were a unified whole. Owing to the Indosinian movement, the eastern NCC uplifted and eroded in the Late Triassic. The Ordos Basin and the Yichuan Basin both received debris from the eastern NCC.

During the Middle-Late Triassic, the northward scissors-type closure of the Mianlue Ocean resulted in an assembly of the South China Block to the Qinling-Dabie Microplate from west to east [61–64]. The Qinling Orogeny belt uplifted rapidly at that time, and has become a stable source area for the southern North China Basin. Meanwhile, Ordos Basin, to the north of the Qinling Orogeny, evolved into a large depression lake basin and preserves a lake facies deposit. Liushan Basin, located in the southern part of the Yichuan Basin, received detrital material from the Qinling orogenic belt in the Middle Triassic [65], which indicates that the Qinling Orogen uplifted in the Middle Triassic. However, the uplift rate of the Qinling Orogen is still minimal in the Middle Triassic. There is a relative balance between the uplift of the mountain and basin subsidence, which maintained an effective state of sedimentary compensation. In the Late Triassic, due to the quick uplift of the Qinling Orogen, the lake basin greatly increased and moved southward significantly. In this study, the Qinling Orogen did not provide provenance for the Yichuan Basin in the Late Triassic. Therefore, we infer that the Funiushan ancient land between the Yichuan Basin and the Liushan Basin was uplifted in the Late Triassic, which hindered the Qinling Orogen from providing material for the Yichuan Basin in the Triassic. Although the Qinling Orogen uplifted in the Late Triassic, it did not provide source material to the Yichuan Basin and only provided source material for the fore-mountain basins (such as the Liushan Basin).

6 Conclusion

Laser ablation inductively coupled plasma mass spectrometry U-Pb dating has been performed on detrital zircons from the Late Triassic Chunshuyao Formation in the Yichuan Basin. The results show three major age groups: 290–252 Ma, 2000–1740 Ma, and 2600–2400 Ma. The lack of Early Paleozoic and Neoproterozoic zircons implies that there is no input from the Qinling Orogen. The detrital zircons of the Chunshuyao Formation may be mainly derived from recycled sediments of the NCC. In the Late Triassic, the Funiu ancient land uplifted and hindered the Qinling Orogen from providing material for the Yichuan Basin.

Acknowledgement: This work was financially supported by the PhD research startup foundation of Guangxi University (XBZ170339), special fund for basic scientific research of central colleges, Chang'an university, China (310827161021). We are grateful to two anonymous reviewers who provided constructive suggestions which led to improvement of the paper.

References

- [1] He M.X., Chang H., Han Y.J., Wu F.Q., Zhao H.Z., The Upper Triassic hydrocarbon accumulation conditions and types in Yichuan basin. *Henan Petroleum*, 1995, 9(3), 17–23 (in Chinese with English abstract)
- [2] Liu S.H., Liu X.N., Li P.H., Characteristics of tectonic evolution and assessment of oil and gas potentiality of the Luoyang-Yichuan basin. *Geology and Resources*, 2003, 12(4), 228–232 (in Chinese with English abstract)
- [3] Li H.W., Mi L.H., Oil controlling structures and exploration prospect analysis on the petroleum in the Yichuan Mesozoic basin, Henan province. *Journal of Henan Polytechnic University (Natural Science)*, 2009, 28(4), 441–444 (in Chinese with English abstract)
- [4] Zheng Q.G., Zhang Y.M., Zhao D.Y., Liu Z.Q., Peng G.L., Tectonic evolution and Upper Triassic distribution in the western Henan. *Henan Petroleum*, 1998, 12(2), 5–10 (in Chinese with English abstract)
- [5] Yan Y.X., Research on gas reservoir characteristics of Triassic dense sandstone in Tun 1 well Yichuan basin and its reservoir forming conditions analysis. *Petroleum Geology and Engineering*, 2013, 27(1), 19–22 (in Chinese with English abstract)
- [6] Liu Y.S., Hu Z.C., Gao S., Günther D., Xu J., Gao C.G., Chen H.H., In situ analysis of major and trace elements of anhydrous minerals by LA-ICP-MS without applying an internal standard. *Chemical Geology*, 2008, 257, 34–43.
- [7] Liu Y.S., Gao S., Hu Z.C., Gao C.G., Zong K.Q., Wang D.B., Continental and oceanic crust recycling-induced melt-peridotite interactions in the Trans-North China Orogen: U-Pb dating, Hf isotopes and trace elements in zircons of mantle xenoliths. *Journal*

- of Petrology, 2010, 51, 537-571.
- [8] Liu Y.S., Hu Z.C., Zong K.Q., Gao C.G., Gao S., Xu J., Chen H.H., Reappraisal and refinement of zircon U-Pb isotope and trace element analyses by LA-ICP-MS. *Chin Sci Bull*, 2010, 55(15), 1535-1546
 - [9] Wiedenbeck M., Alle P., Corfu F., Griffin W.L., Meier M., Oberli F., von Quadt A., Roddick J.C., Spiegel W., Three natural zircon standards for U-Th-Pb, Lu-Hf, trace element and REE analyses. *Geostandards and Geoanalytical Research*, 1995, 19, 1-23
 - [10] Anderson T., Correction of common lead in U-Pb analyses that do not report ^{204}Pb . *Chemical Geology*, 2002, 192, 59-79
 - [11] Ludwig K.R., User's Manual for Isoplot 3.00. A Geochronological Toolkit for Microsoft Excel, Berkeley Geochronology Center, Special Publication No. 4a, Berkeley, CA, 2003
 - [12] Dodson M.H., Compston W., Williams I.S., Wilson J.F., A search for ancient detrital zircons in Zimbabwean sediments. *Journal of the Geological Society*, 1988, 145, 977-983
 - [13] Vermeesch, P., How many grains are needed for a provenance study? *Earth and Planetary Science Letters*, 2004, 224, 441-451
 - [14] Wu Y.B., Zheng Y.F., Genesis of zircon and its constraints on interpretation of U-Pb age. *Chinese Science Bulletin*, 2004, 49, 1554-1569
 - [15] Compston W., Williams I.S., Kirschvink J.L., Zhang Z.C., Guogan M.A., Zircon U-Pb ages for the Early Cambrian time-scale. *Journal of Geological Society, London*, 1992, 149, 171-184
 - [16] Chen F., Zhu X.Y., Wang W., Wang F., Hieu P.T., Siebel W., Single-grain detrital muscovite Rb-Sr isotopic composition as an indicator of provenance for the Carboniferous sedimentary rocks in northern Dabie, China. *Geochemical Journal*, 2009, 43, 257-273
 - [17] Zhu X.Y., Chen F.K., Li S.Q., Yang Y.Z., Nie H., Siebel W., Zhai M.G., Crustal evolution of the North Qinling terrain of the Qinling Orogen, China: Evidence from detrital zircon U-Pb ages and Hf isotopic composition. *Gondwana Research*, 2011, 20, 194-204
 - [18] Lu S.N., Li H.K., Chen Z.H., Hao G.J., Zhou H.Y., Guo J.J., Niu G.H., Xiang Z.Q., Meso-Neoproterozoic Geological Evolution in the Qinling Orogeny and Its Response to the Super-continental Events of Rodinia (in Chinese with English abstract). Beijing: Geological Publishing House, 2003
 - [19] Wang H.L., He S.P., Chen J.L., Xu X.Y., Sun Y., Diwu C.R., LA-ICPMS dating of zircon U-Pb and tectonic significance of Honghuapu subduction-related intrusions in the west segment of Northern Qinling Mountains. *Geosciences*, 2006, 20, 536-544 (in Chinese with English abstract)
 - [20] Wang Q., Zhang H.F., Xu W.C., Cai H.M., Petrogenesis of granites from dangchuan area in West Qinling Orogenic Belt and its tectonic implication. *Earth Science*, 2008, 33, 474-486 (in Chinese with English abstract)
 - [21] Wang T., Wang X.X., Tian W., Zhang C.L., Li W.P., Li S., North Qinling Paleozoic granite associations and their variation in space and time: Implications for orogenic processes in the orogens of central China. *Science China Earth Sciences*, 2009, 52, 1359-1384
 - [22] Wang H.L., Xu X.Y., Chen J.L., Sun Y., Li W.Z., Dating and geochemical characteristics of the Yanwan Paleozoic collisional intrusion in the west segment of Northern Qinling Mountains. *Acta Geologica Sinica*, 2009, 83, 353-364 (in Chinese with English abstract)
 - [23] Li H.Y., He B., Xu Y.G., Huang X.L., U-Pb and Hf isotope analyses of detrital zircons from Late Paleozoic sediments: Insights into interactions of the North China Craton with surrounding plates. *Journal of Asian Earth Sciences*, 2010, 39, 335-346
 - [24] Li P., Chen J.L., Xu X.Y., Wang H.L., Li T., Gao T., Petrogenesis and LA-ICPMS zircon U-Pb dating of the Wuguan intrusive body in North Qinling. *Acta Petrologica et Mineralogica*, 2011, 30, 610-624 (in Chinese with English abstract)
 - [25] Zhang C.L., Liu L., Zhang G.W., Wang T., Chen D.L., Yuan H.L., Liu X.M., Yan Y.X., Determination of Neoproterozoic post-collisional granites in the north Qinling Mountains and its tectonic significance. *Earth Science Frontiers (China University of Geosciences, Beijing)*, 2004, 11, 33-42 (in Chinese with English abstract)
 - [26] Chen Z.H., Lu S.N., Li H.K., Li H.M., Xiang Z.Q., Zhou H.Y., Song B., Constraining the role of the Qinling orogen in the assembly and break-up of Rodinia: Tectonic implications for Neoproterozoic granite occurrences. *Journal of Asian Earth Sciences*, 2006, 28, 99-175
 - [27] Pei X.Z., Ding S.P., Zhang G.W., Liu H.B., Li Z.C., Li W.Y., Liu Z.Q., Meng Y., Zircons LA-ICP-MS U-Pb Dating of Neoproterozoic granitoid gneisses in the north margin of west Qinling and geological implication. *Acta Geologica Sinica*, 2007, 81, 772-786 (in Chinese with English abstract)
 - [28] Wang F., Zhu L.M., Li J.M., Lee B., Gong H.J., Yang T., Wang W., Xu A., Zircon U-Pb ages and Hf isotopic characteristics of the Dehe biotite monzonitic gneiss pluton in the North Qinling orogen and their geological significance. *Chinese Journal of Geochemistry*, 2011, 30, 204-216
 - [29] Zhang G.W., Meng Q.R., Lai S.C., Tectonics and structure of Qinling orogenic belt. *Sciences in China (Series B)*, 1995, 38, 1379-1394
 - [30] Li H.Y., Xu Y.G., Huang X.L., He B., Luo Z.Y., Yan B., Activation of northern margin of the North China Craton in Late Paleozoic: Evidence from U-Pb dating and Hf isotopes of detrital zircons from the Upper Carboniferous Taiyuan Formation in the Ningwu-Jingle basin. *Chinese Science Bulletin*, 2007, 54, 677-686
 - [31] Yang W.T., Yang J.H., Wang X.F., Du Y.S., Geochronology from Middle Triassic to Middle Jurassic detrital zircons in Jiyuan basin and its implications for Qinling orogen. *Earth Science*, 2012, 37, 489-500 (in Chinese with English abstract)
 - [32] Guo J.H., Sun M., Chen F.K., Zhai M.G., Sm-Nd and SHRIMP U-Pb zircon geochronology of high-pressure granulites in the Sanggan area, North China Craton: timing of Paleoproterozoic continental collision. *Journal of Asian Earth Sciences*, 2005, 24, 629-642
 - [33] Darby B.J., Gehrels G., Detrital zircon reference for the North China block. *Journal of Asian Earth Sciences*, 2006, 26, 637-648
 - [34] Gehrels G.E., Yin A., Wang X., Detrital zircon geochronology of the northeastern Tibetan plateau. *Geological Society of America Bulletin*, 2003, 115, 881-896
 - [35] Zhao G.C., Cawood P.A., Wilde S.A., Sun M., Review of global 2.1-1.8 Ga orogens: implications for a pre-Rodinia supercontinent. *Earth Science Reviews*, 2002, 59, 125-162
 - [36] Rogers J.J.W., Santosh M., Tectonics and surface effects of the supercontinent Columbia. *Gondwana Research*, 2009, 15, 373-380
 - [37] Santosh M., Sajeev K., Li J.H., Extreme crustal metamorphism during Columbia supercontinent assembly: evidence from North China Craton. *Gondwana Research*, 2006, 10, 256-266
 - [38] Santosh M., Sajeev K., Li J.H., Liu S.J., Itaya T., Counterclockwise exhumation of a hot orogen: the Paleoproterozoic ultrahigh-temperature granulites in the North China Craton. *Lithos*, 2009,

- 110, 140-152
- [39] Santosh M., Assembling North China Craton within the Columbia supercontinent: the role of double-sided subduction. *Precambrian Research*, 2010, 178, 149-167
- [40] Zhao G.C., Sun M., Wilde S.A., Li S.Z., Late Archean to Paleoproterozoic evolution of the North China Craton: key issues revisited. *Precambrian Research*, 2005, 136, 177-202
- [41] Zhao G.C., Wilde S.A., Guo J.H., Cawood P.A., Sun M., Li X.P., Single zircon grains record two Paleoproterozoic collisional events in the North China Craton. *Precambrian Research*, 2010, 177, 266-276
- [42] Faure M., Trap P., Lin W., Monie P., Bruguier O., Polyorogenic evolution of the paleoproterozoic Trans-North China Belt: new insights from the Luliangshan-Hengshan-Wutaishan and Fuping massifs. *Episodes*, 2007, 30, 96-107
- [43] Trap P., Faure M., Lin W., Monie P., Late Paleoproterozoic (1900–1800Ma) nappe stacking and polyphase deformation in the Hengshan-Wutaishan area: implications for the understanding of the Trans-North-China belt, North China Craton. *Precambrian Research*, 2007, 156, 85-106
- [44] Guo J.H., O'Brien P.J., Zhai M.G., High-pressure granulites in the Sangan area, North China Craton: metamorphic evolution, P-T paths and geotectonic significance. *Journal of Metamorphic Geology*, 2002, 20, 741-756
- [45] Zhao G.C., He Y.H., Sun M., Xiong'er volcanic belt in the North China Craton: implications for the outward accretion of the Paleo-Mesoproterozoic Columbia Supercontinent. *Gondwana Research*, 2009, 16, 170-181
- [46] Zhang S.H., Zhao Y., Song B., Yang Y.H., Zircon SHRIMP U-Pb and in-situ Lu-Hf isotope analyses of a tuff from Western Beijing: Evidence for missing Late Paleozoic arc volcano eruptions at the northern margin of the North China block. *Gondwana Research*, 2007, 12, 157-165
- [47] Zhang S.H., Zhao Y., Song B., Yang Z.Y., Hu J.M., Wu, H., Carboniferous granitic plutons from the northern margin of the North China block: implications for a late Palaeozoic active continental margin. *Journal of the Geological Society*, 2007, 164, 451-463
- [48] Zhang S.H., The Late Paleozoic-Early Mesozoic tectonomagmatic activities in the eastern segment of the Inner Mongolian Uplift in the Yanshan tectonic belt and their geological significance. Ph.D. thesis, Chinese Academy of Geological Sciences, Beijing, 149 p., 2004 (in Chinese with English abstract)
- [49] Zhang S.H., Zhao Y., Liu J., Hu J.M., Chen Z.L., Li M., Pei J.L., Zhou J.X., Emplacement depths of the Late Paleozoic-Mesozoic granitoid intrusions from the northern North China block and their tectonic implications. *Acta Petrologica Sinica*, 2007, 23, 625-638 (in Chinese with English abstract)
- [50] Cope T., Ritts B.D., Darby B.J., Fildani A., Graham S.A., Late Paleozoic sedimentation on the northern margin of the North China Block: implications for regional tectonics and climate change. *International Geology Review*, 2005, 47, 270-296
- [51] Yang J.H., Wu F.Y., Shao J.A., Wilde S.A., Xie L.W., Liu X.M., Constraints on the timing of uplift of the Yanshan Fold and Thrust Belt, North China. *Earth and Planetary Science Letters*, 2006, 246, 336-352
- [52] Tseng C.Y., Yang H.Y., Wan Y.S., Liu D.Y., Da J.W., Lin T.C., Tung K.A., Finding of Neoproterozoic (~775 Ma) magmatism recorded in metamorphic complexes from the North Qilian orogen: Evidence from SHRIMP zircon U-Pb dating. *Chinese Science Bulletin*, 2006, 51, 963-970
- [53] Tung K., Yang H.J., Yang H.Y., Liu D.Y., Zhang J.X., Wan Y.S., Tseng C.Y., SHRIMP U-Pb geochronology of the zircons from the Precambrian basement of the Qilian Block and its geological significances. *Chinese Science Bulletin*, 2007, 52, 2687-2701
- [54] Qin H.P., Petrology of early Paleozoic granites and their relation to tectonic evolution of orogen in the North Qilian Orogenic Belt. Ph.D. thesis, Chinese Academy of Geological Sciences, Beijing, 2012, 141 p. (in Chinese with English abstract)
- [55] Qi J.F., Yu F.S., Lu K.Z., Zhou J.X., Wang Z.Y., Yang Q., Conspectus on Mesozoic basins in Bohai Bay province. *Earth Science Frontiers*, 2003, 10 (Suppl.), 199-206 (in Chinese with English summary)
- [56] Ji Y.L., Hu G.M., Huang J.J., Wu Z.P., Eroded strata thickness of Mesozoic and evolution of Mesozoic and Cenozoic basins in the Bohai Bay basin area. *Acta Geologica Sinica*, 2006, 80(3), 351-358 (in Chinese with English summary)
- [57] Yang M.H., Liu C.Y., Zeng P., Bai H., Zhou J., Prototypes of Late Triassic Sedimentary Basins of North China Craton (NCC) and Deformation Pattern of Its Early Destruction. *Geological Review*, 2012, 58(1), 1-18 (in Chinese with English abstract)
- [58] Chen S.Y., The basin-range coupling in southern North China block during the Late Palaeozoic to Triassic. *Sedimentary Geology and Tethyan Geology*, 2000, 20(3), 37-43 (in Chinese with English abstract)
- [59] Chen S.Y., Sedimentary-Tectonic Evolution from Late Palaeozoic to Triassic in the South of North China Block. *Journal of China University of Mining & Technology*, 2000, 29(5), 536-540 (in Chinese with English abstract)
- [60] Li H.Y., Huang X.L., Constraints on the paleogeographic evolution of the North China Craton during the Late Triassic-Jurassic. *Journal of Asian Earth Sciences* 2013, 70-71, 308-320
- [61] Li S.Z., Zheng Q.L., Li, X.Y., Zhao S.J., Suo Y.H., Guo L.L., Wang Y.M., Zhou Z.Z., Liu X.G., Lan H.Y., Zhang J., Guo R.H., Li S.J., Triassic subduction polarity and orogenic process of the Sulu Orogen, east China. *Marine Geology and Quaternary Geology*, 2017, 37(4), 18-32 (in Chinese with English abstract)
- [62] Peng Z.M., Wu Z.P., Development features of Triassic strata and analysis of original sedimentary pattern in North China. *Geological Journal of China Universities*, 2006, 12(3), 343-352 (in Chinese with English abstract)
- [63] Xia B.D., Li P.J., Sedimentologic evidence on the docking of Yangtze Plate and North China Plate in Middle-Late Triassic period in East China. *Acta Sedimentologica Sinica*, 1996, 14(1), 12-21 (in Chinese with English abstract)
- [64] Li H.G., Du X.D., Lu K.Z., Qi J.F., Tectonic characteristics and evolution of Mesozoic in south and middle Bohai Bay province. *Journal of the University of Petroleum*, 1999, 23(3), 1-5 (in Chinese with English abstract)
- [65] Cao G.S., Yang Q.H., Gao L.X., Lin Y.X., Xing N.N., Zu X.X., Xu G.M., Analysis of sedimentary characteristics and tectonic environment for Late Triassic Liushan Basin. *Chinese Journal of Geology*, 2010, 45(3), 718-733 (in Chinese with English abstract)